

Ligand-Free, Colloidal and Luminescent Metal Sulfide Nanocrystals

Kadlag Kiran,^{†,§} M. Jagadeeswara Rao,^{†,§} Angshuman Nag^{†,*}

[†]Department of Chemistry, Indian Institute of Science Education and Research (IISER), Pune,

India – 411008

[§]Authors contributed equally

*Corresponding author's e-mail: angshuman@iiserpune.ac.in

Supporting Information

Chemicals:

Cadmium oxide (99.995%, Aldrich), 1-dodecanethiol (98%, Aldrich), ammonium sulfide (40-48 wt% solution in water, Aldrich), sulfur (99.998%, Aldrich), formamide (FA, spectroscopy grade, Aldrich), silver Nitrate (99%, Aldrich), toluene (99.5%, Rankem), ethanol (99.9% AR, S D Fine chem. Ltd), N,N-dimethyl formamide (dry S D Fine chem.), cadmium perchlorate hydrate (99.999%,Aldrich), Manganese (II) nitrate hexahydrate (98%, Aldrich), indium (III) nitrate hydrate (99.999%,Aldrich), zinc nitrate hexahydrate (99.999%, Aldrich), N-methyl formamide (99%,Aldrich), toluene(99.8%,Aldrich), 1-Octadecene(90%,Aldrich), dimethylsulfoxide (DMSO, 99.0%, Rankem), acetonitrile (dry, S D Fine chem. Ltd.), didodecyldimethylammonium bromide (DDAB, Aldrich). All the Chemicals were used as received without further purification.

Synthesis:

Ligand-Free CdS Nanocrystals (NCs). In a typical reaction, $\text{Cd}(\text{ClO}_4)_2 \cdot \text{H}_2\text{O}$ (0.2 mmol, 0.0622 g) was dissolved in 10 mL FA in a 50 mL three-neck flask. The flask was heated to 70 °C under N_2 flow, and degassed along with magnetic stirring for about 15 minutes. 100 μL $(\text{NH}_4)_2\text{S}$ solution (40-48% in water) was diluted by adding 1 mL FA and was injected drop by drop to this hot solution. CdS NCs form immediately after the injection of S^{2-} precursor and the reaction was carried out for 15 minutes. The reaction mixture was then cooled to room temperature by removing the heat supply, followed by precipitation and washing of NCs using acetonitrile. These NCs can be dispersed in a suitable polar solvent for solution-based studies, and also can be dried under vacuum at room temperature for powder-based studies.

Ligand-Free $\text{Zn}_x\text{Cd}_{1-x}\text{S}$ NCs. Y mmol of $\text{Zn}(\text{NO}_3)_2 \cdot 6\text{H}_2\text{O}$ and (0.2 - Y) mmol of $\text{Cd}(\text{ClO}_4)_2 \cdot \text{H}_2\text{O}$ was used as a cationic precursor solution in 10 mL FA, such that total cationic precursor is 0.2 mmol. Rest of the synthesis procedures is similar to those of ligand-free CdS NCs.

Ligand-Free Mn-doped $\text{Zn}_x\text{Cd}_{1-x}\text{S}$ NCs. Different amount of Manganese (II) nitrate hexahydrate (0.001, 0.002, 0.003, 0.004, 0.005, or 0.010 mmol) in the range of 0.5 to 5% of 0.2 mmol (Y mmol of $\text{Zn}(\text{NO}_3)_2 \cdot 6\text{H}_2\text{O}$ and (0.2 - y) mmol of $\text{Cd}(\text{ClO}_4)_2 \cdot \text{H}_2\text{O}$) host cationic precursor was added in 10 mL of FA to constitute the cationic solution. Rest of the synthesis procedures is similar to the synthesis of ligand-free CdS NCs.

Ligand-Free AgInS_2 NCs. The cationic solution for AgInS_2 NCs was prepared by dissolving AgNO_3 (0.1 mmol) and $\text{In}(\text{NO}_3)_3 \cdot \text{H}_2\text{O}$ (0.1 mmol) in 10 mL FA. The solution was heated to 70 °C and degassed followed by injection of $(\text{NH}_4)_2\text{S}$ solution, similar to the synthesis of CdS NCs. The reaction was carried out for 15 minutes. The reaction mixture after cooling to room temperature was centrifuged (5000 RPM for 5 minute). The filtrate was collected and heated at 125 °C for 30 minutes under N_2 flow. AgInS_2 NCs can be precipitated by adding acetonitrile.

Oleic Acid Capped CdS NCs. The synthesis was carried following a reported recipe.¹ 0.0496 g CdO, 0.5 mL of oleic acid and 10 mL 1-Octadecene was degassed with nitrogen for at 120 °C for 30 minutes. The reaction mixture was heated up to 300 °C forming a clear solution. 0.016 g sulfur was dissolved in 1 mL 1-octadecene. The sulfur solution is then quickly injected to the Cd solution kept at 300 °C. The reaction was carried out for 30 seconds or 5 minutes. The solution was cooled down to room temperature, diluted with ~10 mL toluene and precipitated by adding excess of ethanol. The precipitates were redispersed in toluene and again precipitated with

acetonitrile, a process that is repeated thrice. The precipitate is dried under vacuum at room temperature.

NC film: NC films are prepared by drop-casting a concentrated solution of NCs on a quartz substrate followed by drying at room temperature. Oleic acid capped NCs were dispersed in hexane, whereas ligand-free NCs were dispersed acetonitrile.

Characterization:

UV-visible absorption and photoluminescence (PL) spectra of NCs were recorded using a Perkin Elmer, Lambda-45 UV/Vis spectrometer and FluoroMax-4 spectrofluorometer (HORIBA scientific), respectively. PL quantum efficiency of NCs were measured by using Rhodamine 6G (QE = 95%) in ethanol as a reference dye. Fourier-transform infrared (FTIR) spectra were acquired in the transmission mode using a NICOLET 6700 FTIR spectrometer (Thermo scientific). Thermogravimetric analysis (TGA) data were measured under inert atmosphere using Perkin Elmer STA 6000, simultaneous thermal analyser. ζ -potential were calculated from measured electrophoretic mobility employing Henry's equation in the Smoluchowski limit,² using a Zetasizer Nano series, Nano-ZS90 (Malvern Instruments, U.K.). Powder x-ray diffraction (XRD) data were collected by using Bruker D8 Advance Powder XRD diffractometer. Transmission electron microscopy (TEM) data were obtained using a JEOL JEM 2100F microscope operated at 200 kV.

Supporting Figures:

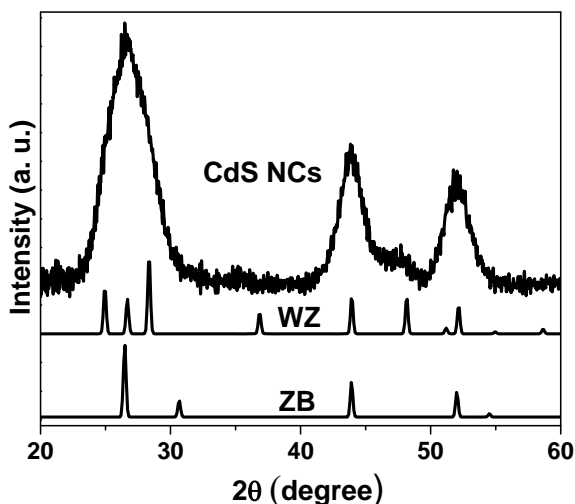


Figure S1: XRD pattern of ligand-free CdS NCs synthesized at 70 °C.

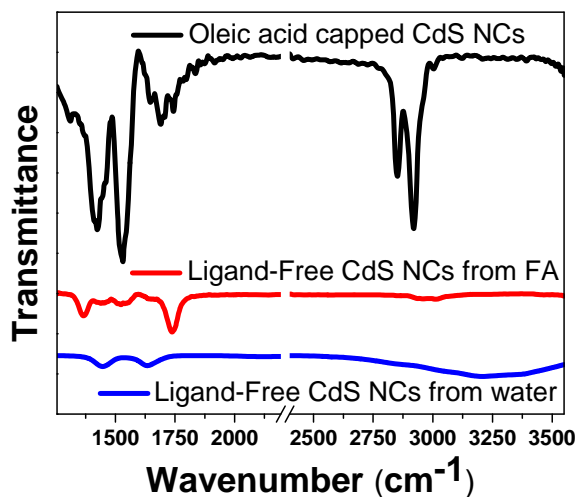


Figure S2: Comparison of FTIR spectra of ligand-free CdS NCs with oleic acid capped CdS NCs. Ligand-free NCs were precipitated from both FA and water.

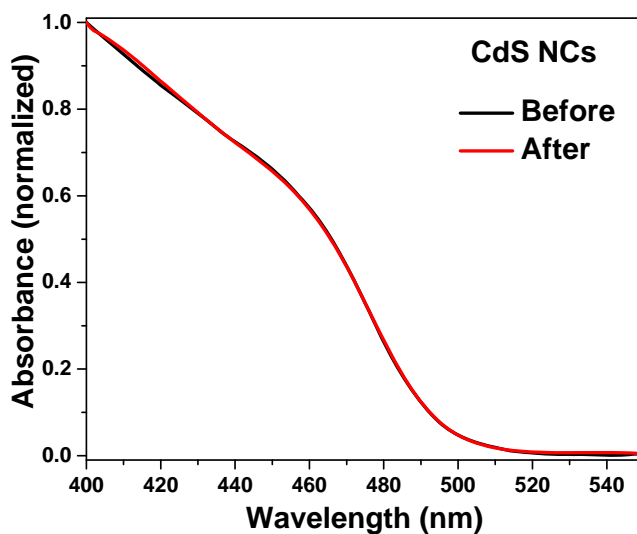


Figure S3: Comparison of UV-visible spectra of ligand-free CdS NCs before and after treating with DDAB. Ligand-free NCs before DDAB treatment were dispersed in formamide and DDAB treated NCs were dispersed in toluene. Both spectra were normalized at their maximum absorbance for a better comparison.

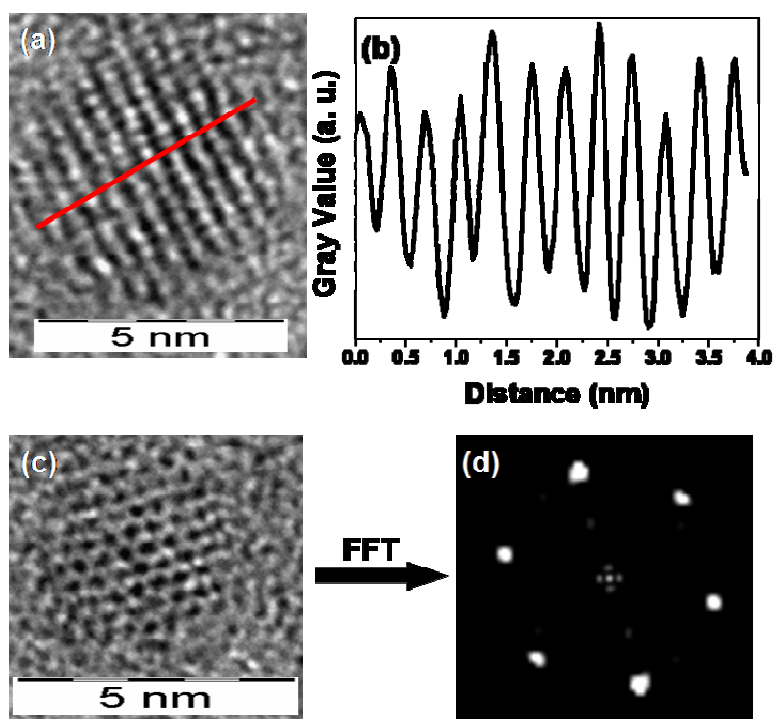


Figure S4: (a) HRTEM image of a DDAB treated ligand-free CdS NC. (b) Gray value intensity line profile of the bright and dark spots along a red line taken from Figure S4a. (c) HRTEM image of another NC taken from the same sample. (d) FFT pattern of the image shown in Figure S4c.

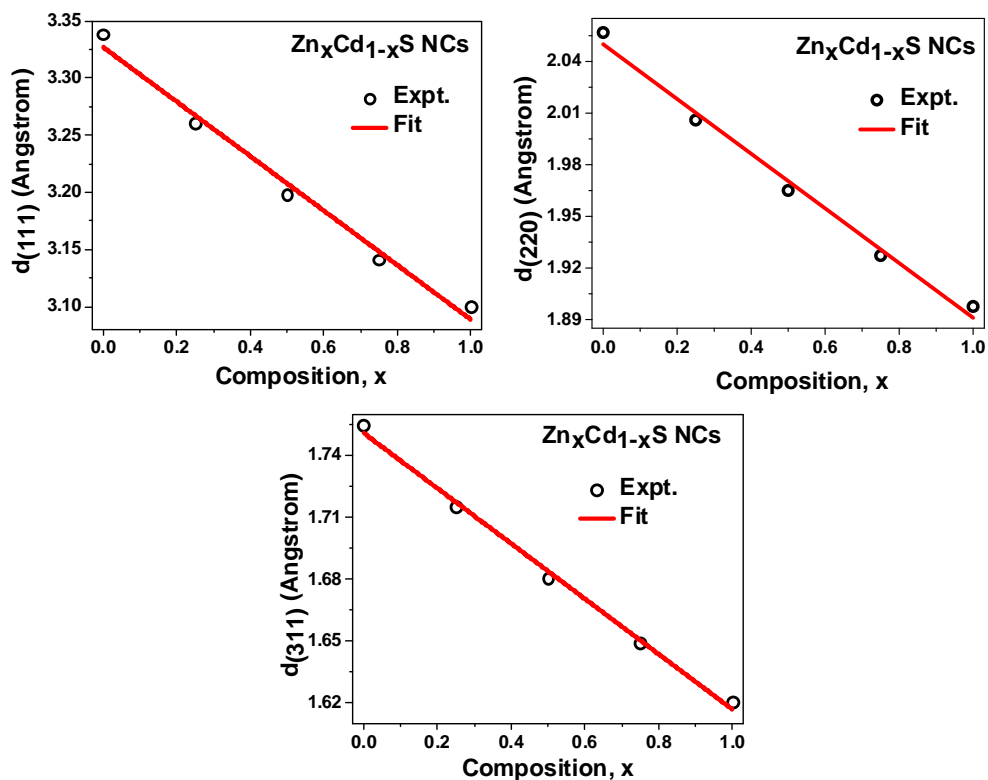


Figure S5: Variation of different interplanar distances (as indicated in the Y-axis label for each plot) with composition “ x ” for the $\text{Zn}_x\text{Cd}_{1-x}\text{S}$ NCs, calculated from their corresponding XRD patterns shown in Figure 3a of the manuscript.

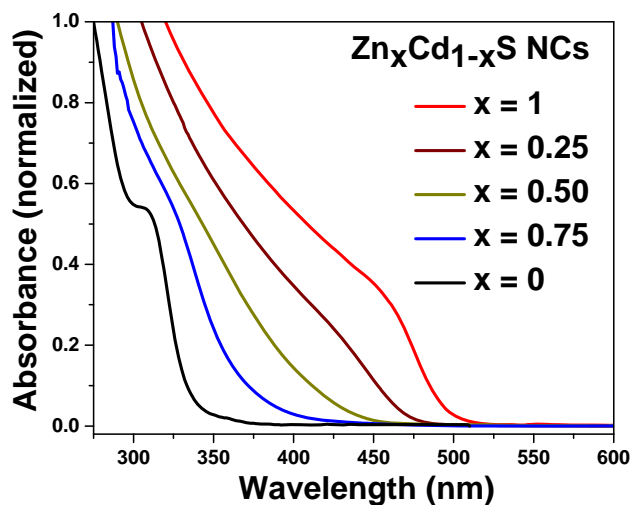


Figure S6: UV-visible absorption spectra of $\text{Zn}_x\text{Cd}_{1-x}\text{S}$ NCs dispersed in formamide. All spectra were normalized at their corresponding maximum absorbance for a better comparison.

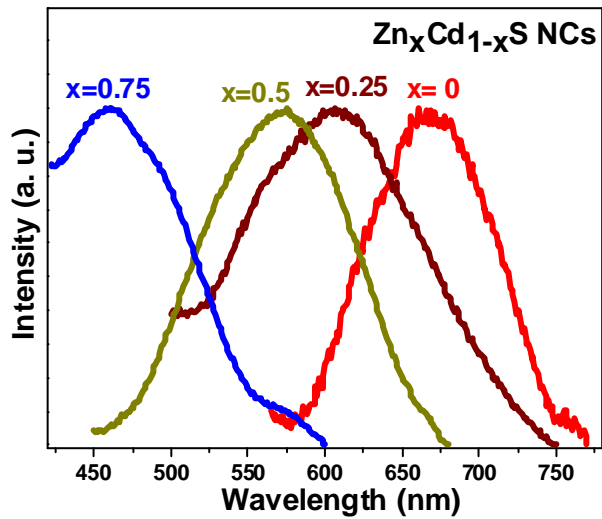


Figure S7: Photoluminescence (PL) spectra of ligand-free $\text{Zn}_x\text{Cd}_{1-x}\text{S}$ NCs dispersed in formamide.

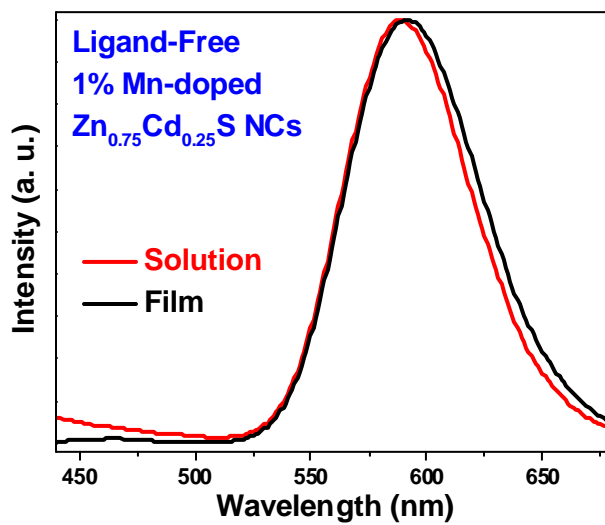


Figure S8: Comparison of PL spectra of ligand-free 1% Mn doped $\text{Zn}_{0.75}\text{Cd}_{0.25}\text{S}$ NCs dispersed in formamide with that of NC film on quartz substrate.

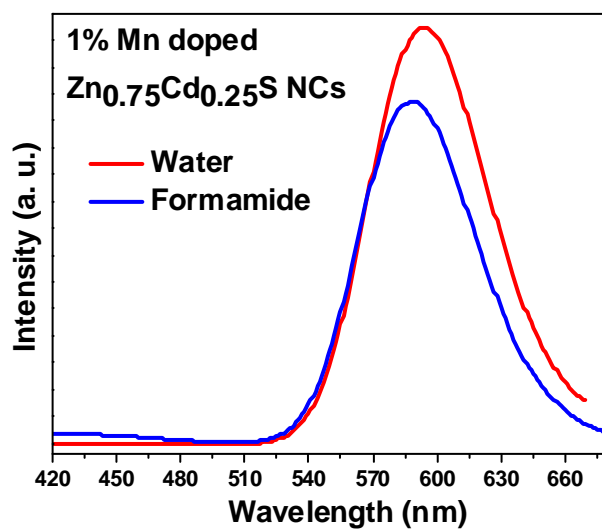


Figure S9: Comparison of PL spectra of 1% Mn doped $\text{Zn}_{0.75}\text{Cd}_{0.25}\text{S}$ NCs dispersed in formamide and water. Water dispersion shows a slight enhancement of Mn emission at the expense surface state emission of the host.

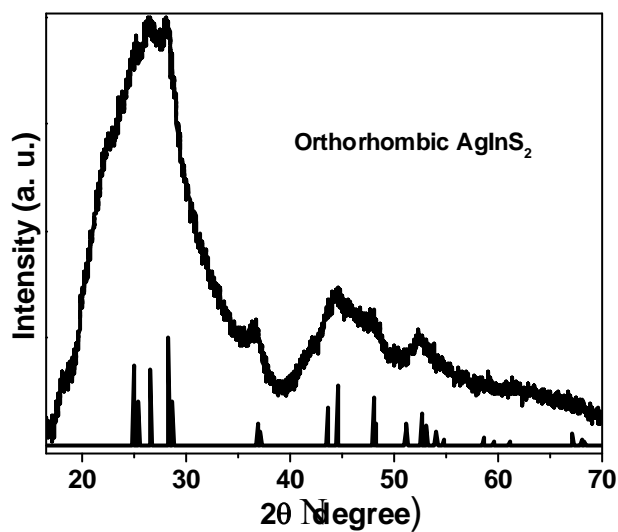


Figure S10: XRD pattern of ligand-free AgInS_2 NCs. Broad pattern is for NCs whereas the sharp lines corresponds orthorhombic phase of bulk AgInS_2 standard.

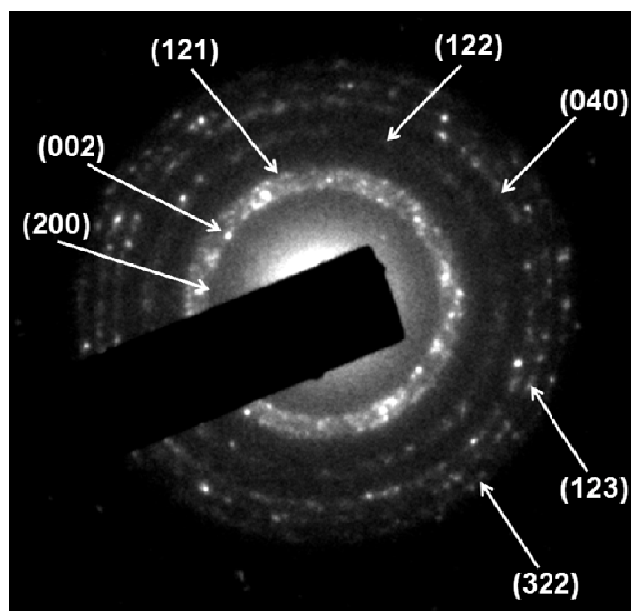


Figure S11: Selected area electron diffraction (SAED) pattern of ligand-free AgInS_2 NCs showing planes corresponding to orthorhombic phase.

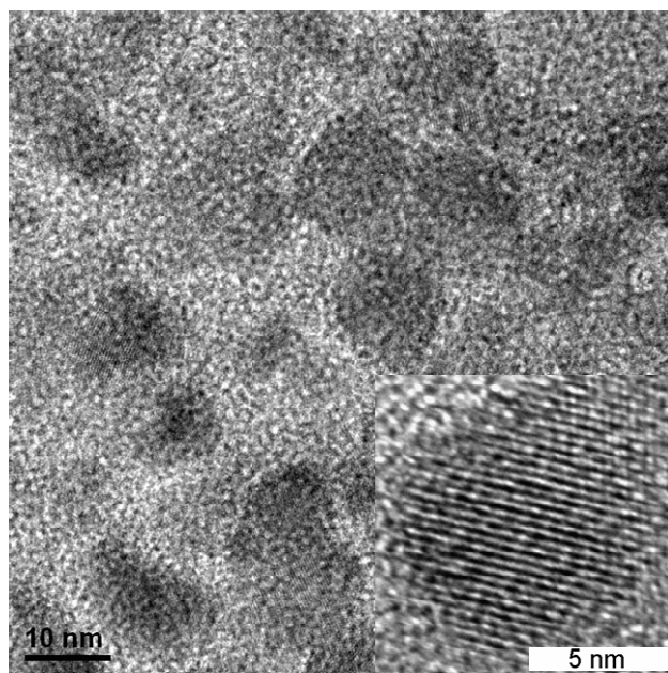


Figure S12: TEM image of ligand-free AgInS_2 NCs. Inset shows HRTEM image of a NC.

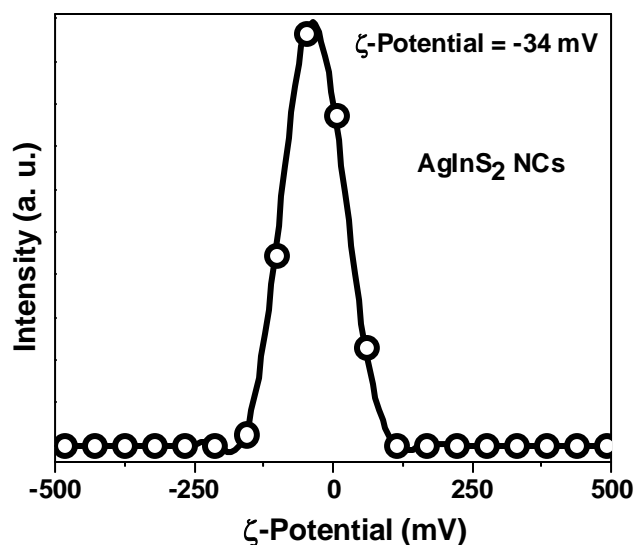


Figure S13: ζ -potential of ligand-free AgInS_2 NCs dispersed in formamide; open circles are experimental data, whereas solid line is a guide to eye.

Electronically Coupled and Luminescent NC Films:

Measuring the electron (hole) mobility by making a field effect transistor (FET) is one of the popular method to quantitatively measure electronic communication in NC films.³ Here we present preliminary qualitative data on possible electronic coupling between adjacent NCs by measuring excitonic absorption of NCs in their dilute dispersion and in close-packed film.⁴ Figure S14a shows that UV-visible absorption spectra of oleic acid capped CdS NCs are similar for both dilute dispersion and film with. However, a red-shift is observed in absorption spectrum of film of ligand-free CdS NCs compared to their dispersion in FA (Figure S14b). Dispersion of ligand-free NCs exhibits an optical gap of 478 nm (2.59 eV), whereas the film exhibit a gap of 487 nm (2.54 eV). Interestingly, redispersing the NC film in FA, reversibly change the absorption spectrum back to the original one with 478 nm optical gap. This reversible red-shift in absorption spectrum of the film of ligand-free NCs suggests possible electronic coupling between adjacent NCs in their film.⁴ In a close packed film of ligand-free NCs, the tail of electronic wavefunctions can spread over multiple adjacent NCs, and consequently, exhibit a red-shift in excitonic absorption. No such red-shift is observed for the film of oleic acid capped NCs because of insulating organic ligand that inhibit spreading of electronic wavefunctions between adjacent NCs. We reemphasize that our results only suggest a possible electronic

coupling between ligand-free NCs, however, transport measurements are required in order to draw an unambiguous conclusion.

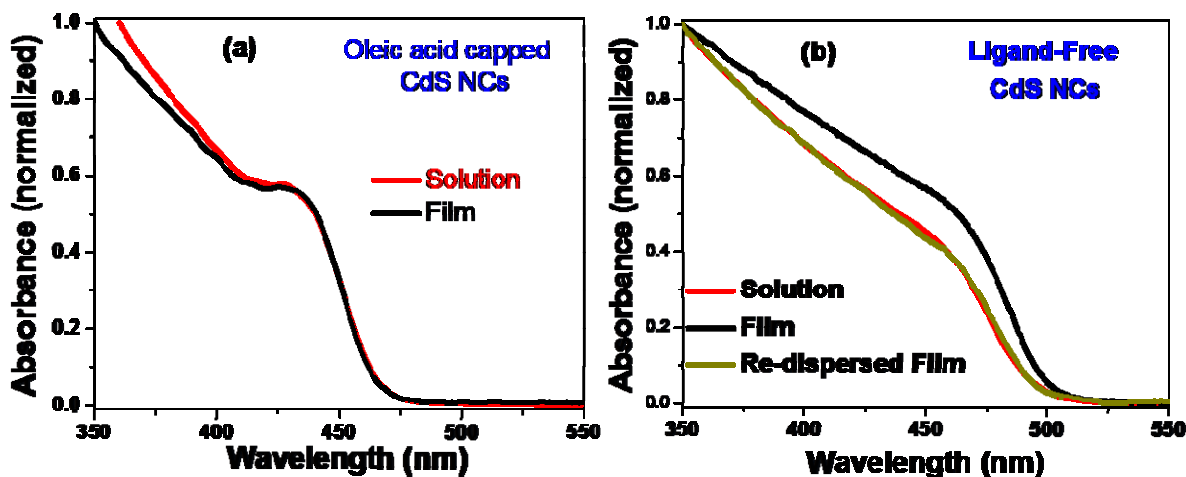


Figure S14: (a) Comparison of UV-visible absorption spectrum of oleic acid capped CdS NCs dispersed in toluene with that of NC film on quartz substrate. (b) Comparison of UV-visible absorption spectra of ligand-free NCs in different forms: formamide solution, film on a quartz substrate, and after redispersing the NC film in formamide.

Film of ligand-free 1% Mn-doped $\text{Zn}_{0.75}\text{Cd}_{0.25}\text{S}$ NCs also exhibit a similar red-shift in absorption spectrum with an optical gap of 349 nm (3.55 eV), compared to their dispersion with optical gap 341 nm (3.63 eV). Interestingly, the film shows strong luminescence similar to their dispersion in FA as shown in Figure S8 and S15. Semiconductor NC films that exhibit good charge transport, often does not exhibit any luminescence, even though the dispersion of same NCs exhibit good luminescence.⁵ This is because of the mutually exclusive requirements, where excitonic emission requires confinement of excitonic wavefunctions within a NC, but electronic coupling requires spreading of the same wavefunctions among adjacent NCs. In the case of our ligand-free Mn-doped NCs, the wavefunctions responsible for luminescence are different from those responsible for charge transport. Inner core Mn^{2+} d states giving luminescence are atomic-like in nature and largely confined within the Mn^{2+} ion, whereas, the charge carriers in the valence band and conduction band of the host can spread over adjacent NCs providing electronic coupling of NCs. However, we must emphasize that further FET-based charge transport studies are required to check the influence of dopant centre on the electron (hole) mobility. Recently, it was shown that the midgap Mn d states in Mn-doped semiconductor NCs helps to improve the

efficiency of NC sensitized solar cells.⁶ In any case, these doped NCs appear to be a potential candidate for future luminescent transistors.

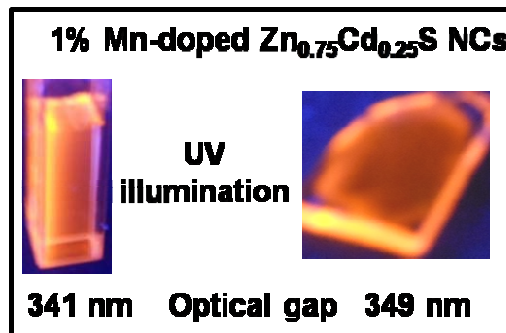


Figure S15: Photographs of luminescence from 1% Mn-doped $\text{Zn}_{0.75}\text{Cd}_{0.25}\text{S}$ NCs in formamide solution and after casting a film on quartz substrate. 365 nm UV light was used to excite the NCs, which is slightly smaller than the optical gap and falls in the tail of absorption spectra.

References:

- (1) Nag, A.; Chakraborty, S.; Sarma, D. D. To dope Mn^{2+} in a Semiconducting Nanocrystal. *J. Am. Chem. Soc.* **2008**, *130*, 10605-10611.
- (2) Pons, T.; Uyeda, H. T.; Medintz, I. L.; Mattoussi, H. Hydrodynamic Dimensions, Electrophoretic Mobility, and Stability of Hydrophilic Quantum Dots. *J. Phys. Chem. B* **2006**, *110*, 20308-20316.
- (3) Lee, J. S.; Kovalenko, M. V.; Huang, J.; Chung, D. S.; Talapin, D. V. Band-Like Transport, High Electron Mobility and High Photoconductivity in All-Inorganic Nanocrystal Arrays. *Nature Nanotechnology* **6** (6), 348-352.
- (4) Kovalenko, M. V.; Scheele, M.; Talapin, D. V. Colloidal Nanocrystals with Molecular Metal Chalcogenide Surface Ligands. *Science* **2009**, *324*, 1417-1420.
- (5) (a) Kovalenko, M. V.; Bodnarchuk, M. I.; Zaumseil, J.; Lee, J. S.; Talapin, D. V. Expanding the Chemical Versatility of Colloidal Nanocrystals Capped with Molecular Metal Chalcogenide Ligands. *J. Am. Chem. Soc.* **2010**, *132*, 10085-10092; (b) Nag, A.; Kovalenko, M. V.; Lee, J. S.; Liu, W. Y.; Spokoyny, B.; Talapin, D. V. Metal-free Inorganic Ligands for Colloidal Nanocrystals: S^{2-} , HS^- , Se^{2-} , HSe^- , Te^{2-} , HTe^- , TeS_3^{2-} , OH^- , and NH_2^- as Surface Ligands. *J. Am. Chem. Soc.* **2011**, *133*, 10612-10620.
- (6) Santra, P. K.; Kamat, P. V. Mn-Doped Quantum Dot Sensitized Solar Cells: A Strategy to Boost Efficiency over 5%. *J. Am. Chem. Soc.* **2012**, *134*, 2508-2511.